Available online at www.sciencedirect.com
SCIENCE DIRECT®
Spectrochimica Acta Part B 59 (2004) 369–374
SPECTROCHIMICA ACTA PART B
www.elsevier.com/locate/sab

Research note

Scanning vs. single spot laser ablation ($\lambda = 213$ nm) inductively coupled plasma mass spectrometry

Jhanis J. González[b], Alberto Fernández[b], Xianglei Mao[a], Richard E. Russo[a,*]

[a]*Lawrence Berkeley National Laboratory, 1 Cyclotron Road, Berkeley, CA 94720, USA*
[b]*Centro de Fisicoquímica Escuela de Química, Universidad Central de Venezuela, Caracas 1020-A, Venezuela*

Received 9 August 2003; accepted 12 December 2003

Abstract

Sampling strategy is defined in this work as the interaction of a repetitively pulsed laser beam with a fixed position on a sample (single spot) or with a moving sample (scan). Analytical performance of these sampling strategies was compared by using 213 nm laser ablation ICP-MS. A geological rock (Tuff) was quantitatively analyzed based on NIST series 610-616 glass standard reference materials. Laser ablation data were compared to ICP-MS analysis of the dissolved samples. The scan strategy (50 μm/s) produced a flat, steady temporal ICP-MS response whereas the single spot strategy produced a signal that decayed with time (after 60 s). Single-spot sampling provided better accuracy and precision than the scan strategy when the first 15 s of the sampling time was eliminated from the data analysis. In addition, the single spot strategy showed less matrix dependence among the four NIST glasses.

Keywords: Laser ablation; Inductively coupled plasma mass spectrometry; NIST glass; Sampling strategy

1. Introduction

Laser ablation inductively coupled plasma-mass spectrometry (LA-ICP-MS) offers many advantages for the analyses of solids samples; among these, pg ml^{-1} detection limits for many elements, wide elemental coverage, a linear dynamic range of up to 10 orders of magnitude, and direct elemental isotopic analysis of solids [1–3]. Successful utilization of LA-ICP-MS involves consideration of a number of parameters. For example, the laser (wavelength, energy, pulse width, beam profile, etc.) [4–8]; the samples and standards (chemical and physical properties, surface condition, availability, etc.) [7,9]; environment surrounding the sample and transport of the material (carrier gas, flow rate, pressure inside the chamber, chamber size, gas dynamic, etc.) [10–13]; and detection system (sensitivity, stability, etc.) [14] all must be optimized to achieve accurate and precise analysis. The influence of these parameters has been summarized in several reviews [1,3,15]. Many investigations have addressed elemental fractionation [1,2,6–8,16–19] as well as numerous parameters for improving chemical analysis performance [13,20–23]. Fractionation has been one of the most difficult effects to eliminate. There are two general types of fractionation experienced during laser ablation, absolute and time dependent. Absolute refers to the case in which the aerosol composition is not chemically matched to the solid sample, for any laser pulse. Time dependent fractionation refers to the case in which the aerosol chemical composition changes during repetitive ablation on the sample (assuming a homogeneous sample).

The sampling strategy governs the ICP-MS time-dependent signal behavior and analytical performance (fractionation, accuracy and precision). Sampling strategies include scanning (raster) mode, and single spot with active focusing or soft ablation [24,25]. The single spot strategy consists of ablating with the laser beam in

*Corresponding author. Tel.: +1-510-486-4258; fax: +1-510-483-7303.
E-mail address: rerusso@lbl.gov (R.E. Russo).

0584-8547/04/$ - see front matter © 2004 Elsevier B.V. All rights reserved.
doi:10.1016/j.sab.2003.12.021

Table 1
Experimental conditions

Laser ablation device	New Wave Research/Merchantek Products. UP-213
Nd:YAG	213 nm (quintupled) 3 ns pulse length
Energy	1.6 mJ
Laser repetition rate	10 Hz
Spot size on the sample	100 μm
Fluence	21 J/cm^2
ICP-MS	PQ3, VG-Elemental
Detector	Simultaneous mode detector
ICP-MS parameters	
RF power	1350 W
Plasma Ar gas flow rate	14.2 l/min
Auxiliary Ar gas flow rate	1.02 l/min
Carrier Ar flow rate	1.3 l/min
ICP-MS Dwell time	10 ms
Data acquisition mode	Time resolved (TRA)

a fixed position on the sample for a period of time. This strategy allows depth profile analyses and provides high spatial resolution when a small spot-size laser beam is used. A disadvantage is fractionation due to crater diameter-to-depth ratio changes [26–28]. The ICP-MS temporal response using single spot sampling initially shows higher signal intensity, followed by stabilization of the signal due to conditioning of the sample. This change in temporal behavior has been related to changes in particle size distribution during crater formation [20,21,29]. Generally, the initial few seconds of the signal cannot be used for analysis; integration of the signal has to be performed after a pre-ablation time.

The scanning strategy involves moving the sample (at a fixed speed) while the laser beam is repetitively pulsed. This strategy has been shown to reduce time dependant variations in the signal intensity related to crater formation. Flat response with time or constant mass ablation rate also is beneficial for optimizing ICP-MS conditions (lens voltages, torch position, etc.). According to the definition by Fryer et al. [26], the ratio of different elements having flat response leads to a fractionation index near 1. Although a fractionation index of 1 indicates no time dependent fractionation, it does not necessarily translate to improved signal precision or quantitative analysis.

This paper describes a comparative study (qualitative and quantitative) of these two sampling strategies (single spot vs. scanning) using 213 nm laser ablation. NIST 610-616 glasses were used to compare the precision associated with each sampling strategy. For quantitative analysis, a geological sample (Tuff rock) was ablated using both strategies and calibrated using the NIST glasses as standards. The data were compared to solution results for the dissolved rock sample.

Table 2
Tuff characteristics and element reference concentrations

Mineralogical composition abundance	Species	Concentration from solution analysis
Cristobalite	SiO_2	76.44%
Anorthoclase	CaO	0.53%
Sanidine	Pb	27 ± 1 ppm
Wustite	Th	21.4 ± 1 ppm
	U	2.3 ± 0.2 ppm

2. Experimental

The experimental system has been described previously [6]. All laser and ICP-MS conditions are listed in Table 1. The ablation was performed in argon gas to emphasize the effects of larger particles during initial ablation. The Tuff (volcanic) rock sample was chosen because of its similar composition to the NIST glass series. Activation Laboratories LTD in Canada previously analyzed this sample; the composition and characteristics of the Tuff rock are listed in Table 2.

The single spot strategy consisted of ablating in a fix position on the sample for 1 min with the laser operating at 10 Hz. This procedure was repeated three to five times (in separate spots). The scan strategy consisted of translating the laser beam across the samples with a speed of 50 μm/s for 1 min. For this case, three separate positions were scanned (1, 2 and 3) and three scans were made for each position (A, B and C). Fig. 1 shows profiles (interferometer microscope) in NIST 610 after scans A, B and C at scan position 1. For both strategies the laser beam spot size was 100 μm. The analysis time was 60 s (signals measured for 550 laser shots).

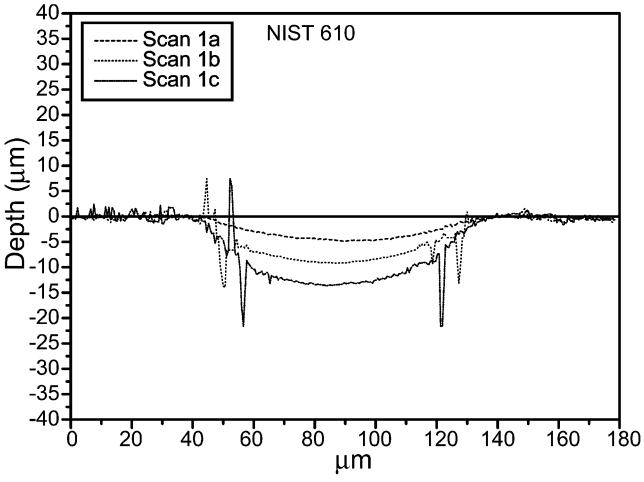

Fig. 1. Profiles (interferometer microscope) in NIST 610 after scans A, B and C at scan position 1.

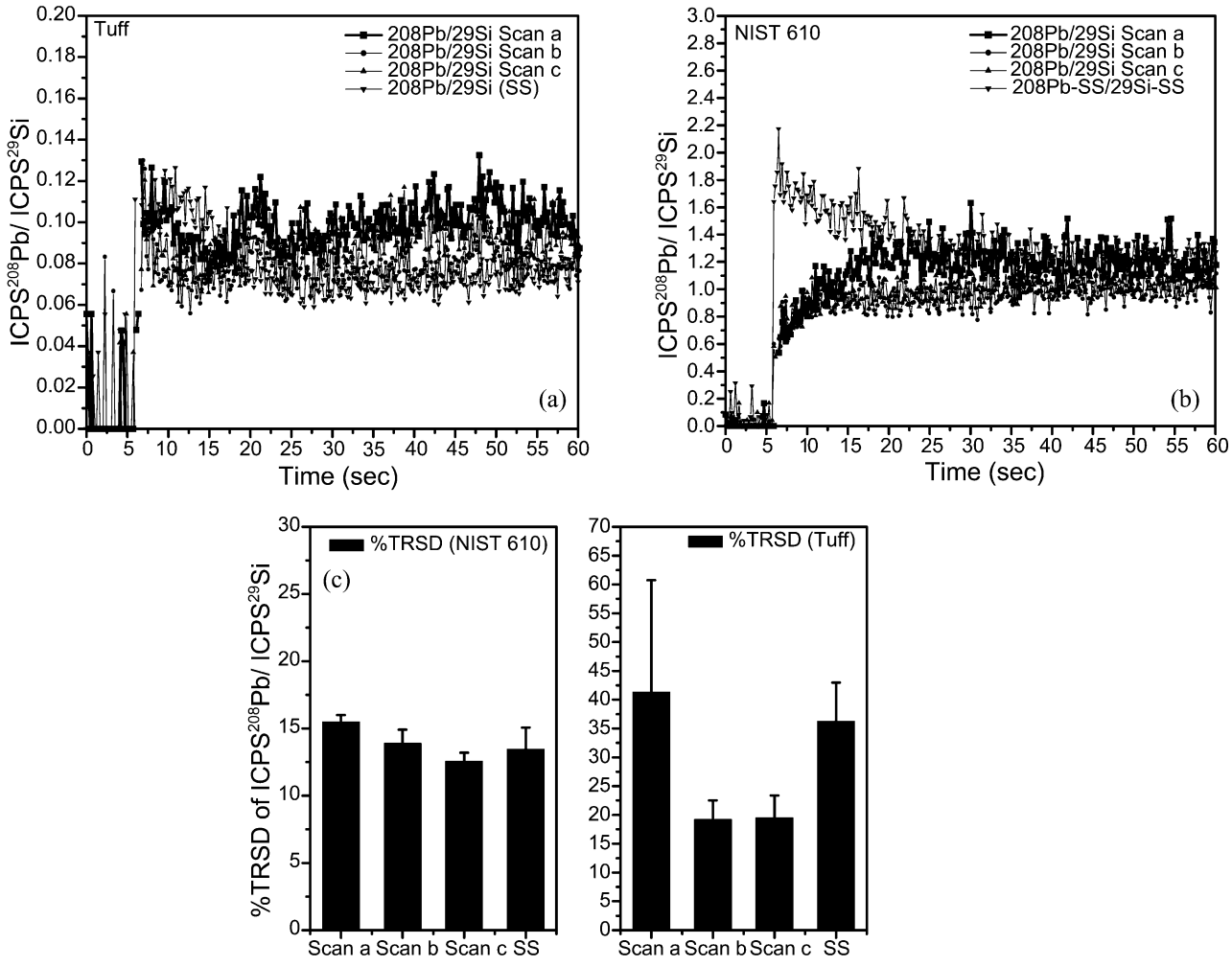

Fig. 2. The temporal signal intensity ratios $^{208}Pb/^{29}Si$ produced by the sampling strategies single spot and scan: (a) Tuff, (b) NIST 610 and (c) temporal relative standard deviation (% TRSD) of the signals from NIST 610 and Tuff.

3. Results and discussions

ICP-MS temporal $^{208}Pb/^{29}Si$ ratios from NIST 610 and Tuff during single spot and scanning ablation are shown in Fig. 2a,b, respectively. There are two components to these data that affect analytical performance, the long-term change in intensity representing the long-term change in the amount of mass ablated, and the short-term intensity fluctuations due to pulse-to-pulse sampling imprecision. The data using homogeneous NIST 610 glass demonstrate the differences using the two sampling strategies. The single spot data are initially high with a subsequent slow decay, sometimes requiring minutes to reach a steady level. The long-term behavior represents the change in amount of mass ablated as the crater is formed. The exact behavior is a complicated relationship between laser and sample properties [20,29]. The scanning strategy produces a steady state level within a few seconds, especially noticed for scans B and C in Fig. 2b. Scan A is affected by impurities and defects (scratches) on the sample surface, whereas scans B and C represent a sample surface that is somewhat conditioned by previous laser pulses.

The temporal relative standard deviation (TRSD) of the signal is related to the short-term change, and was calculated by dividing the standard deviation of the signal average (after subtracting the background) by the signal-integrated value, for each sample position. Scan A shows poorer TRSD in the $^{208}Pb/^{29}Si$ ratio (Fig. 2c) than scans B and C for both NIST 610 and especially the tuff sample.

The fractionation index (FI) is related to the long-term change in the signal intensity. To compute the fractionation index, the total temporal signal (55 s) was divided in two parts, 1st part from 5 to 27.5 s and the 2nd part from 27.5 to 55 s. FI is defined as the ratio of the silicon normalized signal in the 2nd part (27.5–55 s) of the acquisition divided by the silicon normalized

Table 3
Fractionation index for ^{208}Pb relative to ^{29}Si

	FI	FI	FI
NIST-scans	(A)1.1±0.2	(B)1.05±0.02	(C)1.05±0.06
NIST-ss	0.94±0.04		
Tuff-scans	(A)1.1±0.1	(B)1.0±0.1	(C)1.0±0.2
Tuff-ss	1.1±0.1		

Table 4
Correlation coefficients (R) for the calibration curves obtained for both sampling strategies

	SS	Scan A	Scan B	Scan C
Pb	0.9983	0.9961	0.9970	0.9983
Pb/Si	0.9999	0.9993	0.9965	0.9978
Pb/Ca	0.9999	0.9978	0.9956	0.9992

Table 5
Values calculated for parameters of the calibration curves (Log $Y = A + B$ Log X)

	A	B
Pb-SS	2.86±0.06	0.97±0.04
Pb-scan A	3.09±0.11	0.89±0.06
Pb-scan B	3.05±0.10	0.81±0.04
Pb-scan C	3.06±0.06	0.85±0.04
Pb/Si-SS	3.02±0.02	1.01±0.01
Pb/Si-scan A	2.78±0.21	0.93±0.04
Pb/Si-scan B	2.92±0.21	1.02±0.06
Pb/Si-scan C	2.68±0.20	0.94±0.04
Pb/Ca-SS	2.44±0.03	1.00±0.01
Pb/Ca-scan A	2.56±0.11	0.99±0.03
Pb/Ca-scan B	2.52±0.23	0.99±0.03
Pb/Ca-scan C	2.31±0.12	0.96±0.03

signal in the first part (5–27.5 s). Table 3 presents the FI values for ^{208}Pb relative to ^{29}Si. Both sampling strategies gave a value very close to 1 indicating no relative fractionation to Si. Similar data were obtained for ^{232}Th and ^{238}U.

Calibration curves were established for lead (^{208}Pb), thorium (^{232}Th) and uranium (^{238}U). For comparison purpose, the signals produced by both sampling strategies were integrated after a time of 15 s. Two elements were used as internal standards (^{29}Si and ^{44}Ca). These calibrations curves were used to quantify Pb, Th and U in the Tuff rock sample. Linear fitting to the experimental data provided standard deviation and regression coefficients listed in Tables 4 and 5. Improved regression coefficients and lower standard deviation values for the slope and the intercept were measured using the single spot strategy over the scan strategy. Again, similar data were measured for ^{232}Th and ^{238}U.

Table 6
Results obtained for concentration of ^{208}Pb, ^{232}Th and ^{238}U using the single spot sampling strategy

Calibration curve used	Element	Ref. value	LA value single pot	%Diff. to ref	%R.S.D.
Pb	Pb	27±1	35.6±2.6	32	7
Pb/Si	Pb	27±1	26.9±3.2	0	12
Pb/Ca	Pb	27±1	29.7±10.7	10	36
Th	Th	21.4±1	35.1±2.4	64	7
Th/Si	Th	21.4±1	23.1±1	8	4
Th/Ca	Th	21.4±1	23±1.7	7	8
U	U	3.9±0.2	10.4±0.4	166	4
U/Si	U	3.9±0.2	5.2±0.2	33	3
U/Ca	U	3.9±0.2	6.1±0.6	56	10

Tables 6 and 7 show the Pb, Th and U concentration in Tuff sample computed using the calibration curves described above. The relative standard deviation (%R.S.D.) represents the reproducibility of the data from one spot to another. The use of silicon (Si) as an internal standard provided better accuracy than calcium (Ca) because the Si distribution in the Tuff sample is homogeneous, which is not the case for Ca. Even when Si was used as a standard, the best data were obtained using the single spot strategy.

The temporal signal intensity ratios for ^{208}Pb/^{29}Si measured from NIST 610 (Fig. 2a) were 1.292±0.098 using the single spot strategy, while the average using

Table 7
Results obtained for concentration of ^{208}Pb, ^{232}Th and ^{238}U using the scan sampling strategy

Calibration curve used	Element	Ref. value	LA value scan A	%Diff. to ref	%R.S.D.	LA value scan B	%Diff. to ref	%R.S.D.	LA value scan C	%Diff. to ref	%R.S.D.
Pb	Pb	27±1	38.9±19.5	44	50	47.6±10.2	76	21	43.9±5	63	11
Pb/Si	Pb	27±1	25.5±13.1	−6	51	36.9±4.6	37	12	34.2±5	27	15
Pb/Ca	Pb	27±1	76.6±38.8	184	51	110.7±19.3	310	17	117.6±16.8	336	14
Th	Th	21.4±1	43.5±13.5	103	31	39.2±7.5	83	19	32.1±6.1	50	19
Th/Si	Th	21.4±1	26.9±8.7	26	32	25.4±4.8	19	19	23.6±4	10	17
Th/Ca	Th	21.4±1	69.2±1.6	223	2	77.8±13.7	264	18	167±17	−22	10
U	U	3.9±0.2	13.7±4.1	252	30	13.6±2.2	248	16	5.8±1	48	18
U/Si	U	3.9±0.2	5.3±1.9	35	36	11.6±1.9	199	16	5.3±0.8	36	15
U/Ca	U	3.9±0.2	13.2±1.2	239	9	5.7±1	46	18	13.7±1.2	252	9

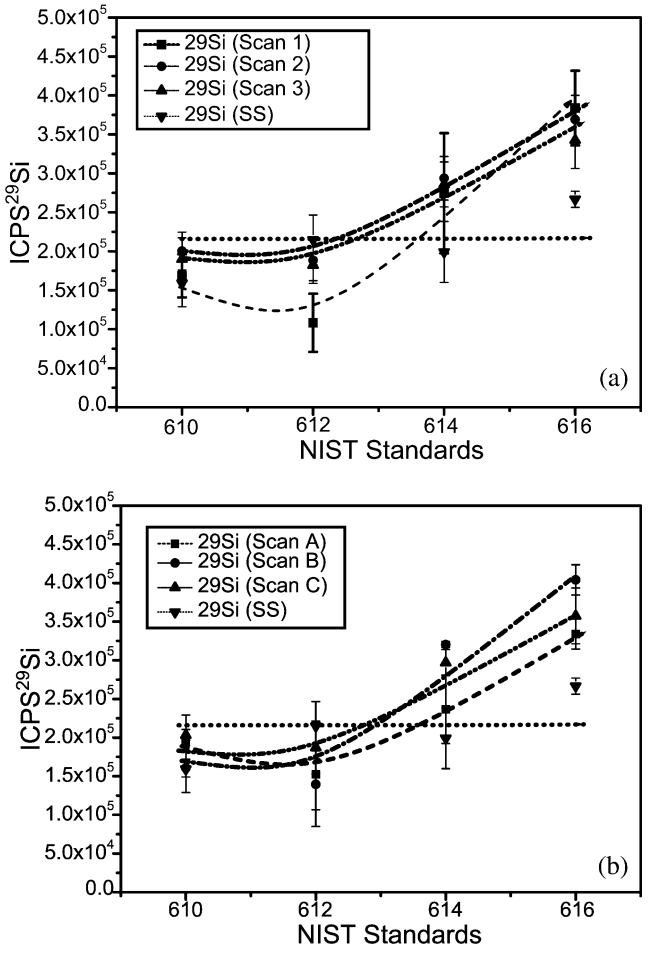

Fig. 3. ^{29}Si signal intensity vs. sample number (opacity 610 ≫ 616); (a) comparison single spot vs. average of scans 1, 2 and 3; (b) comparison single spot vs. average of scans A, B and C.

the scan strategy was 1.086 ± 0.158. Although the nominal value for this ratio in the ICP was not established, this behavior demonstrates how sampling parameters can influence ICP-MS measurements. This change is attributed solely to the sampling strategy, because the samples and ICP-MS conditions were constant. Differences in the particle size distribution (not measured) for these two sampling strategies may be responsible for the difference in measured ratio and analytical performance [13,20,21].

Another difference from these two sampling strategies is shown in Fig. 3a,b. The matrix element (^{29}Si) is present in the four NIST glass samples at the same concentration. The single spot strategy provided less matrix dependence as shown in the ICP-MS intensity measurements compared to the scanning strategy, even for scans B and C.

4. Conclusion

Single spot vs. sample scanning at 50 μm/s were compared for analytical precision and accuracy using laser ablation ICP-MS. The single spot strategy showed better accuracy (compared to results by liquid dissolution of the sample) and precision (%R.S.D.) than the scanning strategy (50 μm/s) for the quantification of ^{208}Pb, ^{232}Th and ^{238}U in a Tuff rock sample. The difference in the performance is related to the reproducibility of the laser sampling process, primarily the conditioning of the sample surface by successive laser pulses. Si gave better results than Ca as the internal standard due to its homogeneity in the Tuff sample. The temporal relative standard deviation (%T.R.S.D.) of the temporal ratio ^{208}Pb/^{29}Si showed higher values for scan A and single spot sampling than for scan B and C in the NIST 610 and Tuff samples. The calculated fractionation index showed no significant fractionation of ^{208}Pb to ^{29}Si and no significant difference for both sampling strategies.

Acknowledgments

The US Department of Energy, Office of Basic Energy Sciences, Chemical Sciences Division, and the Office of Nonprol iteration and National Security (NA22) supported this research at the Lawrence Berkeley National Laboratory under Contract No DE-AC03-76SF00098. J.J. Gonzalez also thanks the CDCH of the Central University of Venezuela.

References

[1] S.F. Dun-ant, J. Anal. Atom. Spectrom. V15 (1999) 1385–1403.
[2] D. Gunther, I. Horn, B. Hattendorf, Fresenius. J. Anal. Chem. 368 (2000) 4–14.
[3] R.E. Russo, X.L. Mao, H.C. Liu, J. Gonzalez, S. S. Mao, Talanta V57 (2002) 425–451.
[4] H.C. Liu, O.V. Borisov, X.L. Mao, S. Shuttleworth, R.E. Russo, Appl. Spectrosc. 54 (2000) 1435–1442.
[5] M. Guillong, I Horn, D. Gunther, J. Anal. Atom. Spectrom. 18 (2003) 1224–1230.
[6] J. Gonzalez, X.L Mao, J. Roy, S. Mao, R.E. Russo, J. Anal. Atom. Spectrom. 17 (2002) 1108–1113.
[7] T.E. Jeffries, S.E. Jackson, H.P. Longerich, J. Anal. Atom. Spectrom. V13 (1998) 935–940.
[8] D. Gunther, R. Frischknecht, C.A. Heinrich, H.J. Kahlert, J. Anal. Atom. Spectrom. V12 (1997) 939–944.
[9] X.L. Mao, W.T. Chan, R.E. Russo, Appl. Spectrosc. 57 (1997) 1047–1054.
[10] R. E. Russo, X.L Mao, M. Caetano, M.A Shannon, Appl. Surf. Sci. 96–98 (1996) 144–148.
[11] W.T. Chan, A.P.K. Leung, X.L. Mao, R.E. Russo, Appl. Surf. Sci. V129 (1998) 269–273.
[12] A.P.K. Leung, W.T. Chan, X.L. Mao, R.E. Russo, Anal. Chem. V70 (1998) 4709–4716.
[13] I. Horn, D. Gunther, Appl. Surf. Sci. 207 (2003) 144–157.
[14] M. Ducreux-Zappa, J.M. Mermet, Spectrochim. Acta Part B 51 (1996) 333–341.
[15] D. Gunther, S.E. Jackson, H.P. Longerich, Spectrochim. Acta Part B 54 (1999) 381–409.
[16] J.S. Becker, D. Tenzler, Fresenius. J. Anal. Chem. 370 (2001) 637–640.

[17] I. Horn, M. Guillong, D. Gunther, Appl. Surf. Sci. 182 (2001) 91–102.
[18] M.E. Taylor, D.L. Blaney, G. Cardell, Appl. Surf. Sci. V165 (2000) 166–177.
[19] A. Semerok, C. Chaleard, V. Detallc, J.L. Lacour, P. Mauchien, P. Meynadier, C. Nouvellon, B. Salle, P. Palianov, M. Perdrix, G. Petite, Appl. Surf. Sci. V739 (1999) 311–314.
[20] S.H. Jeong, O.V. Borisov, J.H. Yoo, X.L. Mao, A.E. Russo, Anal. Chem. 77 (1999) 5123–5130.
[21] M. Guillong, D. Gunther, J. Anal. Atom. Spectrom. 2002.
[22] J. Koch, I. Feldmann, N. Jakubowski, K. Niemax, Spectrochim. Acta Part.B-Atom. Spectrosc. 57 (2002) 975–985.
[23] Z Pászti, Z.E Horváth, G. Peto, A. Karacs, L. Guczi, Appl. Surf. Sci. 109–110 (1997) 67–73.
[24] T. Hirata, J. Anal. Atom. Spectrom. V12 (1997) 1337–1342.
[25] W.T. Perkins, N.J.G. Pearce, J.A. Westgate, Geostandards Newsl.-J Geostandards Geoanalysis 21 (1997) 175–190.
[26] B.J. Fryer, S.E. Jackson, H.P. Longerich, Can. Mineral. V33 (1995) 303–312.
[27] S.M Eggins, L.P.J. Kinsley, J.M.G. Shelley, Appl. Surf. Sci. 127–129 (1998) 278–286.
[28] D. Gunther, C-A. Heinrich, J. Anal. Atom. Spectrom. 14 (1999) 1363–1368.
[29] O.V. Borisov, X.L. Mao, R.E. Russo, Spectrochim. Acta Part B 55 (2000) 1693–1704.